JOURNAL OF NATURAL PRODUCTS

pubs.acs.org/jnp

Article

Synthesis and Biological Evaluation of Falcarinol-Type Analogues as Potential Calcium Channel Blockers

Yang Li,[#] Wan-Li Tan,[#] Kai Guo, Xiao-Wei Gao, Jun Wei, Dong Yi, Chun Zhang,* and Qin Wang*

Cite This: https://doi.org/10.1021/acs.jnatprod.1c00136

Read Online

ACCESS | Metrics & More | Article Recommendations | Supporting Information

ABSTRACT: A series of enantiomers of falcarinol analogues (**2**) were synthesized using a chiral 1,1′-binaphth-2-ol (BINOL)-based catalytic system. The neuroprotective effects of falcarinol (**1a**) and its analogues (**2**) on PC12 cells injured by sodium azide (NaN_3) were investigated. The structure−function relationships and possible mechanism were studied. Pretreatment of PC12 cells with falcarinol analogues (*R*)-**2d** and (*R*)-**2i** for 1 h following addition of NaN_3 and culture in a CO_2 incubator for 24 h resulted in significant elevation of cell viability, as determined by a CCK-8 assay and Hoechst staining, with reduction of LDH release and MDA content, increase of SOD activity, and decrease of ROS stress, when compared with the activity of natural falcarinol (**1a**). These observations indicated that the falcarinol analogues (*R*)-**2d** and (*R*)-**2i** can protect PC12 cells against NaN_3-induced apoptosis via increasing resistance to oxidative stress. For the first time, falcarinol (**1a**) and its analogue (*R*)-**2i** were found to have potential L-type calcium channel-blocking activity, as recorded using a manual patch clamp technique on HEK-293 cells stably expressing *h*Cav1.2 (α1C/β2a/α2δ1). These findings suggest that the mechanism of the L-type calcium channel-blocking activity of falcarinol (**1a**) and its analogue (*R*)-**2i** might be involved in neuroprotection by falcarinol-type analogues by inhibiting calcium overload in the upstream of the signaling pathway.

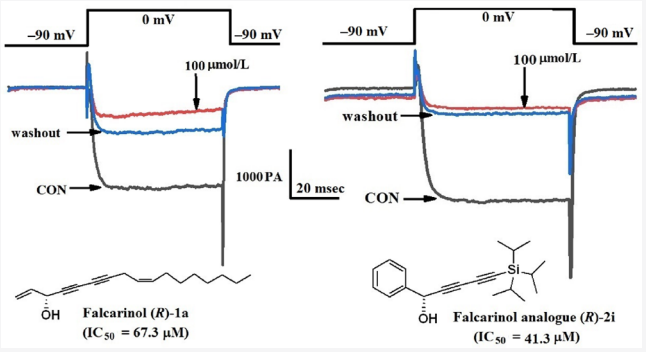

Falcarinol (**1a**) is a C_{17} polyacetylenic chiral alcohol with the *R*-configuration, which is distributed widely in food plants belonging to the family Apiaceae (e.g., carrots, celery, parsnips, and coriander) and also in medicinal plants from the family Araliaceae (e.g., *Panax ginseng* and *Panax notoginseng*).[1] The polyacetylenic falcarinol-type compounds are characterized by a conjugated diyne-carbinol structural motif and a long hydrocarbon chain and have been reported to possess different bioactivities.[2,3] Due to its lipophilic nature and rapid absorption in humans, compound **1a** is believed to have potential neuroprotective and neurotrophic effects since it may cross the blood−brain barrier and enter the brain.[4] Lu et al. reported the neurotrophic effects of **1a** on PC12 cells and the mechanism involved in the neurite outgrowth of these cells.[5] Furthermore, the protective effect of **1a** on sodium nitroprusside (SNP)-induced neuronal apoptosis was investigated in primary cultured cortical neurons.[6] The potential mechanism suggested that **1a** can protect neurons against exogenous nitric oxide (NO)-induced toxicity via regulating apoptotic and antiapoptotic proteins, where the deleterious effects of NO production have been associated with neurodegenerative conditions such as Alzheimer's disease (AD).[6] The protective effect of **1a** on Aβ_{25-35}-induced neuronal apoptosis was also verified, and its antiapoptotic mechanism involved the inhibition of calcium influx and free-radical generation.[7] These results raise the possibility that **1a** might reduce neurodegeneration in the AD brain. Compound **1a** was also identified as a reversible agonist of the cannabinoid receptor CB1 and is capable of selectively alkylating the anandamide binding site.[8] Falcarindiol (**1b**), with two stereogenic hydroxy groups, was found to show a potent allosteric modulatory action on $GABA_A$ receptors, possibly by modulating agonist binding and desensitization, but **1a** possessed a higher affinity for $GABA_A$ receptors and also a substantially different pharmacological action than **1b**.[9,10] Oenanthotoxin (**1c**) and dihydrooenanthotoxin (**1d**), with fully conjugated diyne-diene moieties and delocalized hydroxy groups, were both found to show a complex blocking mechanism of $GABA_A$ receptors.[11] The inhibitory effects of **1c** and **1d** on GABAergic currents are strongly dependent on polarity.[12] These findings indicate that falcarinol-type analogues might affect the functioning of the central nervous system by interfering with receptors for key neurotransmitters. L-Type calcium channels mainly exist in the cell body of central neurons and proximal dendrites. The

Received: February 9, 2021

mechanism of calcium homeostasis suggests that the calcium disturbances in AD could lead to calcium overloading in the mitochondria, which results in the opening of mitochondrial permeability-transition pores and the release of calcium stored.[13,14] Accordingly falcarinol (**1a**) and its analogues also may interact with L-type calcium channels as potential targets for treating calcium dysregulation.

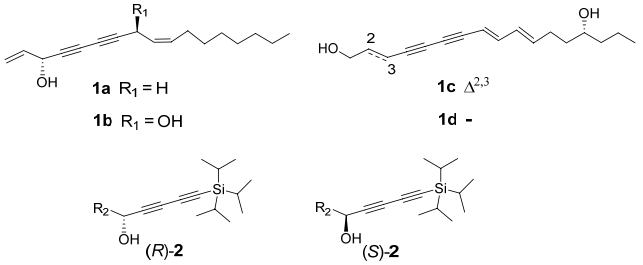

Our group recently conducted the asymmetric synthesis of several chiral falcarinol analogues, (*R*)-**2**, with a conjugated diynol moiety and a triisopropylsilyl (TIPS) group, using a chiral amino alcohol [(1*S*,2*S*)-2-*N*,*N*-dimethylamino-1-(*p*-nitrophenyl)-3-(*tert*-butyldimethylsilyloxy)propan-1-ol)]-based catalytic process, which exhibited potential antiproliferative activity against certain cancer cell lines.[15] Several optically active falcarinol analogues were also prepared using this chiral 1,1′-binaphth-2-ol (BINOL)-based catalytic system.[15−17] Since the TIPS (C_9 + Si) group of these compounds is lipophilic, similar to that of the linear chain (C_{10}) of falcarinol (**1a**), these falcarinol analogues also may possess neuroprotective effects. In the present study are reported the asymmetric synthesis of (*R*)- and (*S*)-falcarinol analogues **2** with (*S*)- or (*R*)-BINOL-based catalysts, the neuroprotective effects of **1a** and its analogues **2** against NaN_3-induced toxicity on PC12 cells, structure−function relationships, and mechanistic investigations including lactate dehydrogenase (LDH) release, malondialdehyde (MDA) content, superoxide dismutase (SOD) activity, and reactive oxygen species (ROS) stress, as well as the potential calcium channel-blocking activity.

RESULTS AND DISCUSSION

(*R*)- and (*S*)-Falcarinol analogues **2a−p** were synthesized using the readily available C_2-symmetric (*S*)- and (*R*)-BINOL ligand system, to catalyze the asymmetric addition of TIPS-substituted 1,3-diyne to a variety of aromatic and aliphatic aldehydes, as shown in Scheme 1. The catalysis using BINOL in combination with $Ti(O^iPr)_4$, Zn powder, and EtI avoids the direct use of the spontaneously combustible $ZnEt_2$, making it possible to conduct a much safer operation in large scale of industrial production under very mild reaction conditions.[15,18] This method was applied to the preparation of falcarinol analogues in this investigation for the first time. As shown in Table 1, the optically active conjugated diynecarbinols with a phenyl group, including *ortho*-, *meta*-, or *para*-substituents, were obtained in excellent enantioselectivities and high yields (entries 1−11). High enantioselectivities and high yields were observed for the addition of a TIPS-substituted alkyne to α-branched aliphatic aldehydes and α,β-unsaturated aldehydes (Table 1, entries 12−16). The *R*- or *S*-configuration of each product was determined by comparing the optical rotation and HPLC data with literature values (Table 1).[15,19,20]

The rat PC12 pheochromocytoma cell line is a well-established model for the investigation of neuronal cell responses of differentiation, proliferation, and survival. It was reported that falcarinol (**1a**) has neuroprotective effects on PC12 cells.[5] An excess of NO is viewed as a deleterious factor involved in various neurodegenerative disorders.[21,22] In the present study, a model of PC12 cell injury induced by NaN_3 as a NO donor was established using a CCK-8 assay. The survival rate of PC12 cells exhibited a dose-dependent relationship with NaN_3, as shown in Figure S1, Supporting Information. When PC12 cells were treated with 0 and 36 mM NaN_3 for 24 h, their survival rates were about 100% in the control group and 50% in the model group. As shown in Table S1, Supporting Information, pretreatment of the cells with 1−32 μM falcarinol (**1a**) for 1 h following addition of NaN_3 and culturing in a CO_2 incubator for 24 h resulted in an increase of cell viability, and 2−8 μM falcarinol (**1a**) protected well PC12 cells from injury by NaN_3, with a ca. 59% survival rate, while higher concentrations (16 and 32 μM) of **1a** led to a gradual decrease in its protective effect.

Next, the protective effects of (*R*)- and (*S*)-falcarinol analogues **2a−p** against NaN_3-induced toxicity on PC12 cells were investigated using an established CCK-8 assay. These results of cell viability from 32 samples at various concentrations (5, 10, 20, 40, 80, 100 μM) are listed in Table S2, Supporting Information, as the treatment group relative to the control group and the model group. As shown in

Scheme 1. Asymmetric Synthesis of (*R*)- and (*S*)-Falcarinol Analogues 2 Using the (*S*)- and (*R*)-BINOL-Based Catalytic System

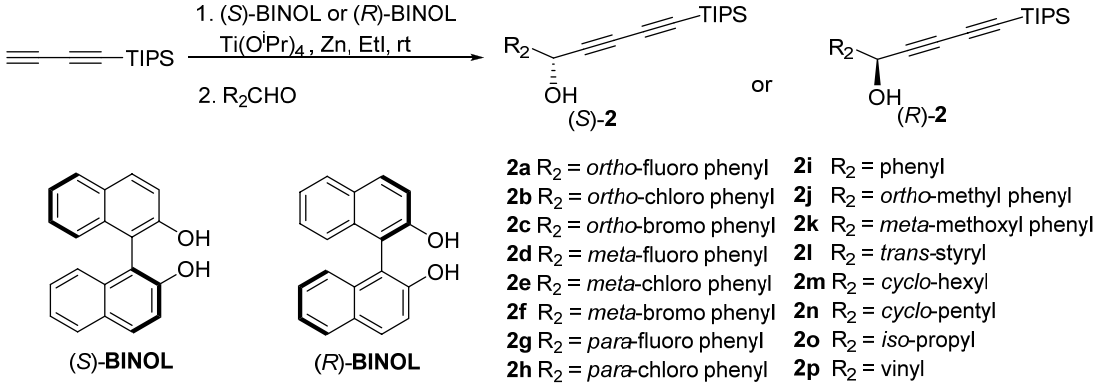

https://doi.org/10.1021/acs.jnatprod.1c00136
J. Nat. Prod. XXXX, XXX, XXX−XXX

Table 1. Products (2a−p) from Asymmetric Addition of Diynes to Aldehydes in the Presence of (*S*)- and (*R*)-BINOL

entry	BINOL	product **2**	yield (%)	ee (%)	$[\alpha]_D^{20}$
1	(*R*)	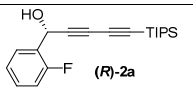 **(*R*)-2a**	70	91	+26.3
	(*S*)	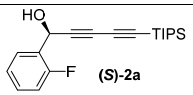 **(*S*)-2a**	60	96	-25.5
2	(*R*)	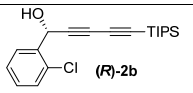 **(*R*)-2b**	71	93	+60.9
	(*S*)	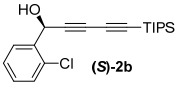 **(*S*)-2b**	63	92	-58.6
3	(*R*)	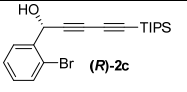 **(*R*)-2c**	74	91	+68.0
	(*S*)	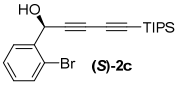 **(*S*)-2c**	69	91	-67.4
4	(*R*)	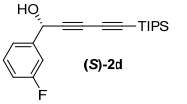 **(*S*)-2d**	61	94	+8.6
	(*S*)	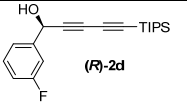 **(*R*)-2d**	60	96	-8.8
5	(*R*)	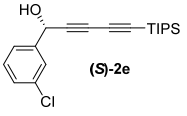 **(*S*)-2e**	80	94	+7.3
	(*S*)	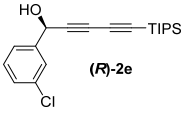 **(*R*)-2e**	80	97	-7.5
6	(*R*)	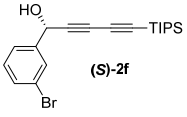 **(*S*)-2f**	91	98	+5.9
	(*S*)	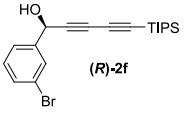 **(*R*)-2f**	60	98	-5.7
7	(*R*)	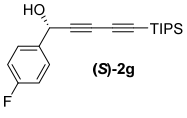 **(*S*)-2g**	70	94	+28
	(*S*)	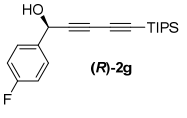 **(*R*)-2g**	68	93	-28.6

https://doi.org/10.1021/acs.jnatprod.1c00136
J. Nat. Prod. XXXX, XXX, XXX−XXX

Table 1. continued

entry	BINOL	product **2**	yield (%)	ee (%)	$[\alpha]_D^{20}$
8	(*R*)	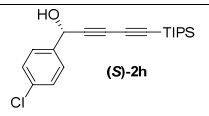 **(*S*)-2h**	62	97	+9.9
	(*S*)	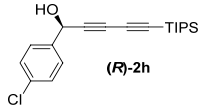 **(*R*)-2h**	66	99	-9.6
9	(*R*)	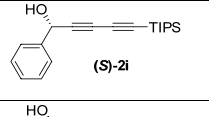 **(*S*)-2i**	65	94	+6.0
	(*S*)	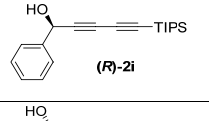 **(*R*)-2i**	62	94	-6.3
10	(*R*)	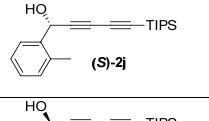 **(*S*)-2j**	77	98	+32.5
	(*S*)	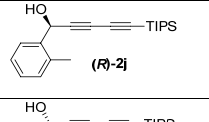 **(*R*)-2j**	72	97	-20.9
11	(*R*)	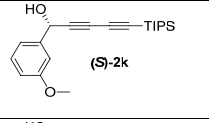 **(*S*)-2k**	89	97	+8.5
	(*S*)	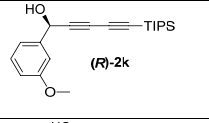 **(*R*)-2k**	89	95	-8.8
12	(*R*)	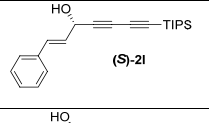 **(*S*)-2l**	82	92	+29.7
	(*S*)	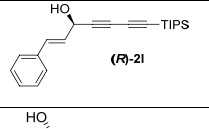 **(*R*)-2l**	84	92	-29.3
13	(*R*)	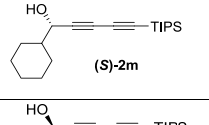 **(*S*)-2m**	86	92	+8.6
	(*S*)	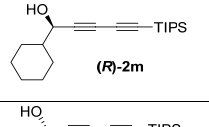 **(*R*)-2m**	75	87	-8.1[a]
14	(*R*)	 **(*S*)-2n**	95	90	+16.8
	(*S*)	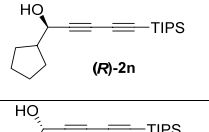 **(*R*)-2n**	85	90	-16.7
15	(*R*)	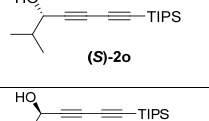 **(*S*)-2o**	73	95	+3.9
	(*S*)	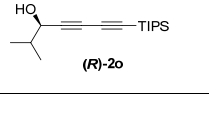 **(*R*)-2o**	91	93	-3.3

https://doi.org/10.1021/acs.jnatprod.1c00136
J. Nat. Prod. XXXX, XXX, XXX−XXX

Table 1. continued

entry	BINOL	product **2**	yield (%)	ee (%)	$[\alpha]_D^{20}$
16	(*R*)	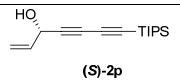 **(*S*)-2p**	73	89 [b]	+38.4
	(*S*)	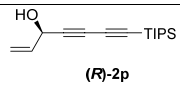 **(*R*)-2p**	78	90 [b]	-38.3

[a]The *R*-configuration of the product was determined by comparing the optical rotation and HPLC data with literature values.[15,19,20] [b]Each ee value was determined by ^{1}H NMR spectroscopy after using a chiral derivatization reagent (see Supporting Information).

Table S2, 32 falcarinol analogues exhibited different cell viabilities relative to the control group, and lower concentrations (5−10 μM) of **2**, in general, gave higher cell survival rates. Compared with the falcarinol (**1a**) positive control group (Table S1, Supporting Information), the analogues (*R*)-**2d** and (*R*)-**2i** had better neuroprotective effects on the injured cell model, with 83% (76%) and 60% (67%) cell viabilities at 5 μM (10 μM) (Table S3, Supporting Information). In addition, the individual analogues (*R*)-**2k** and (*R*)-**2n** also exhibited neuroprotective activities at a higher concentration of 20 μM (40 μM), with 61% (65%) and 66% (65%) cell viabilities (Table S3, Supporting Information).

The cell viabilities of falcarinol analogues **2** and possible structure−activity relationships were compared (Figure 1). In Figure 1A, the benzene ring-substituted analogues (*R*)-**2i** resulted in higher cell viabilities than the vinyl, styryl, and α-branched aliphatic substituted analogues **2l−p** at 5 μM. In turn, the aromatic-substituted analogues **2a−k**, (*R*)-**2d**, with a *meta*-fluoro substituent, displayed higher neuroprotective effects for PC12 cells injured by NaN_3 than compounds **2a** and **2g**, with either an *ortho*- or *para*-fluoro substituent, as shown in Figure 1B, in addition to compounds **2e**, **2f**, and **2k** containing a *meta*-chloro, bromo, or methoxy group in the phenyl ring. Comparison of both enantiomers of certain falcarinol analogues demonstrated that (*R*)-**2d**, (*R*)-**2i**, and (*R*)-**2k** gave much greater survival rate values in the injured PC12 cell model than their opposite enantiomers (*S*)-**2d**, (*S*)-**2i**, and (*S*)-**2k**, as shown in Figure 1C.

It has been reported that falcarinol (**1a**) not only exhibits neuroprotective effects on injured cortical neurons but also promotes neurite outgrowth and the expression of the differentiation marker of PC12 cells.[5−7] Thus, the neurotrophic effects of falcarinol (*R*)-**1a** and its analogues, (*R*)-**2d**, (*R*)-**2i**, and (*R*)-**2k**, on PC12 cells were investigated by their cell viability index in the CCK-8 assay. As shown in Table S4 (Supporting Information), the falcarinol analogues, (*R*)-**2d**, (*R*)-**2i**, and (*R*)-**2k**, exhibited dose-dependent neurotrophic effects on PC12 cells in a manner similar to that of falcarinol (**1a**). At low concentrations (1−10 μM), analogues (*R*)-**2d**, (*R*)-**2i**, and (*R*)-**2k** gave cell survival rates of 81−96% at 24 h, among which (*R*)-**2i** exhibited the best neurotrophic effects on PC12 cells, with a cell viability rate up to 96% at a concentration of 1 μM.

Given the relationship between its lipophilic structure and neurotrophic effects of (*R*)-**2i**, the neuroprotective effects were tested of the falcarinol analogues (*R*)-**2i** and (*R*)-**3** and the falcarindiol analogue (*R,R*)-**6** in the injured PC12 cell models by removal of the lipophilic TIPS (C_9 + Si) group of (*R*)-**2i** and replacement with a C_{10} linear aliphatic chain. As shown in Table 2, the low cellular viability for analogue (*R*)-**3** (48−52%) confirmed that the lipophilic group is indispensable for the neuroprotective effects of analogues (*R*)-**2i** (60−67%) and (*R,R*)-**6** (64−66%), with ether a TIPS group or a linear aliphatic chain under low concentration levels (5−10 μM). Moreover, analogue (*R*)-**2i**, with a TIPS group (52−58%), led to a higher potential for cell survival than (*R,R*)-**6**, with a linear aliphatic chain (31−52%), at high concentration levels (40−100 μM). Additionally, (*R*)-**2i**, containing a benzene ring, also displayed a higher neuroprotective effect than (*R*)-**4** and (*R*)-**5**, containing a C_{10} linear aliphatic chain, as a synthetic intermediate of the falcarindiol analogue (*R,R*)-**6** (Figure S2b, Supporting Information).

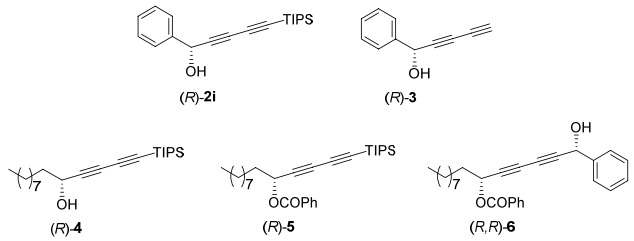

Hoechst staining was performed to visualize the extent of cell apoptosis. The neuroprotective effects of (*R*)-**2d** and (*R*)-**2i** on apoptotic PC12 cells induced by NaN_3 was determined by Hoechst 33258 staining (Figure S3, Supporting Information). As shown in Figure 2, the falcarinol analogue (*R*)-**2d** at concentrations of 5 and 10 μM attenuated NaN_3-induced apoptosis of PC12 cells, and the percentage of positively stained cells showed good consistency and hallmarks of apoptotic death such as chromatin condensation and fragmentation.

Lactate dehydrogenase release into the medium is a good indicator of the degree of cellular damage. The neuroprotective effects of falcarinol (**1a**) and its analogues, (*R*)-**2d** and (*R*)-**2i**, on NaN_3-induced PC12 cell death was investigated using an LDH release assay (Table S5, Supporting Information). As shown in Figure 3, the PC12 cell injury induced by NaN_3 resulted in a significant LDH release (412 or 417 U/L). Pretreatment with falcarinol (**1a**) (4 μM) reduced the LDH release to 211 U/L. Concentration of analogues (*R*)-**2d** and (*R*)-**2i** from 5 to 10 μM lowered NaN_3-induced toxicity in PC12 cells with LDH release from 132 to 270 U/L, and analogue (*R*)-**2i** at 5 μM protected PC12 cells from NaN_3-induced toxicity with an LDH content down to 132 U/L.

It has been reported that falcarinol (**1a**) can also alleviate early-stage neuronal degeneration induced by the toxic fragment of fibril $A\beta_{25-35}$. Its mechanism involved the inhibition of intracellular free-radical generation and extracellular calcium overload.[7] Several studies have shown that NO-

https://doi.org/10.1021/acs.jnatprod.1c00136
J. Nat. Prod. XXXX, XXX, XXX−XXX

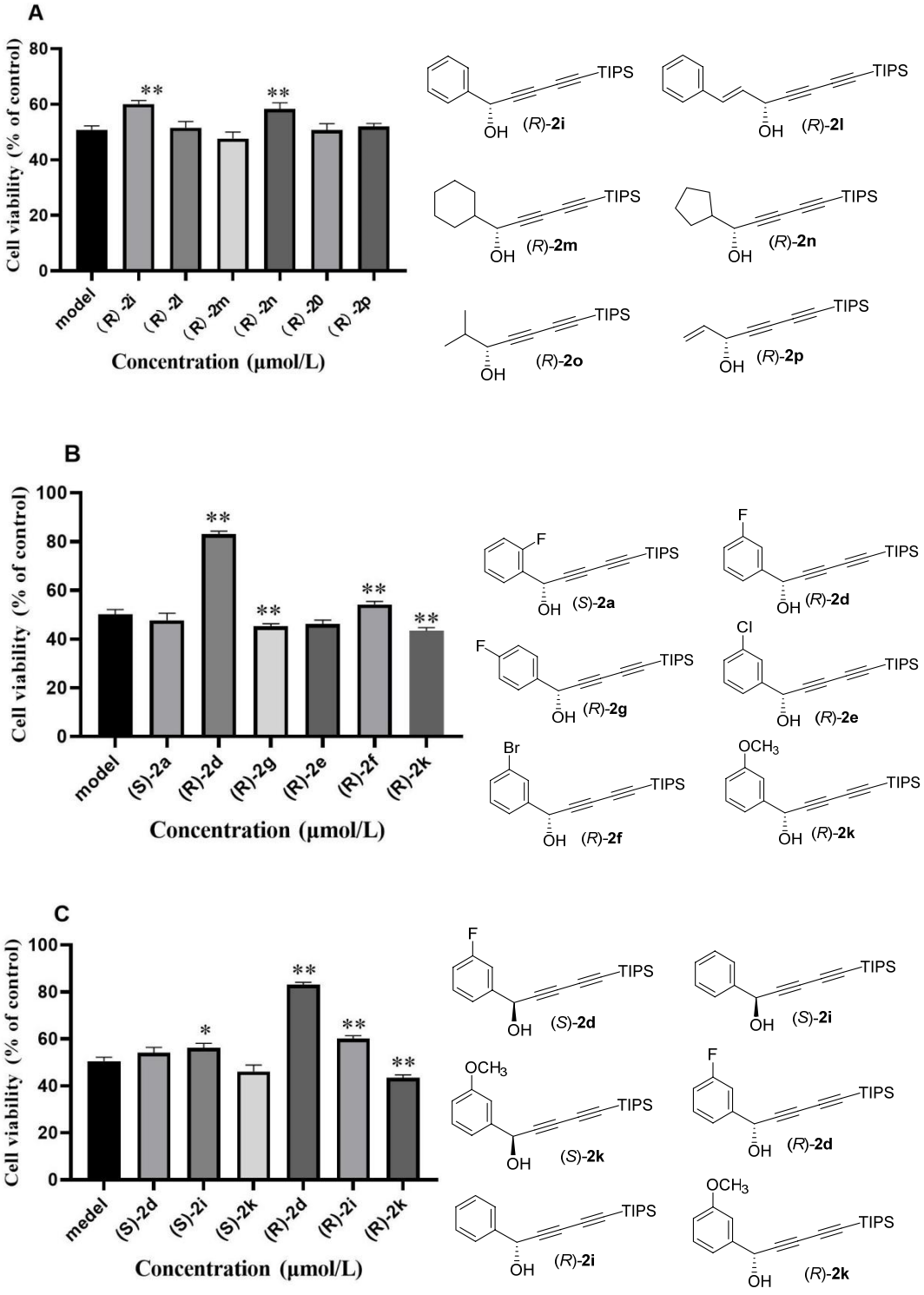

Figure 1. Cell viability of the falcarinol analogues **2** and their structure−activity relationships. (A) Aromatic-substituted (*R*)-**2i** and aliphatic-substituted **2l**−**p**; (B) aromatic substituents containing *ortho*-, *meta*-, and *para*-fluoro phenyl groups, **2a**, **2d**, and **2g**, and containing an electron-withdrawing group in the *meta*-position, **2e**, **2f**, and **2k**; (C) aromatic-substituted (*S*)-**2d**, (*R*)-**2d**, (*S*)-**2i**, (*R*)-**2i**, (*S*)-**2k**, and (*R*)-**2k**. x ± s, $n = 3$. $^{*}p < 0.05$, $^{**}p < 0.01$ vs model group.

induced toxicity engendered by its reaction with the superoxide anion radical yields the highly cytotoxic ROS peroxynitrite.[21] Peroxynitrite then decomposes to form nitrogen dioxide and hydroxyl radicals, leading to lipid peroxidation, protein oxidation, and DNA damage.[22] MDA has been studied extensively as an indicator of lipid peroxidation with manifestations of oxygen toxicity. As shown in Figure 4, a significant increase of MDA levels (253 nmol/mL) compared to the control group was observed in a model group of PC12 cell injury induced by NaN_3. Pretreatment with the analogues (*R*)-**2d** and (*R*)-**2i** at a concentration of 5 μM decreased greatly the content of MDA

https://doi.org/10.1021/acs.jnatprod.1c00136
J. Nat. Prod. XXXX, XXX, XXX−XXX

Table 2. Effects of Various Concentrations of Analogues (*R*)-2i, (*R*)-3, (*R*)-4, (*R*)-5, and (*R,R*)-6 on PC12 Cell Injury Induced by NaN_3[a]

analogue	control	model	5 μM	10 μM	20 μM	40 μM	80 μM	100 μM
(*R*)-**2i**	100 ± 2.2[b]	49.9 ± 1.0	60.1 ± 1.2[b]	66.6 ± 2.5[b]	58.0 ± 1.8[b]	58.2 ± 2.9[b]	53.0 ± 1.5	51.9 ± 1.3
(*R*)-**3**	100 ± 0.7	51.5 ± 2.1	47.8 ± 2.1	52.4 ± 2.5	55.0 ± 1.2	49.9 ± 1.5	47.5 ± 1.2	43.5 ± 1.5[b]
(*R*)-**4**	100 ± 1.8	50.0 ± 1.0	49.4 ± 0.8	47.8 ± 1.2	46.2 ± 2.4	43.5 ± 1.8[b]	39.5 ± 1.4[b]	37.6 ± 1.6[b]
(*R*)-**5**	100 ± 0.9	50.6 ± 0.5	50.4 ± 1.0	47.9 ± 1.3	47.5 ± 1.2	46.4 ± 0.6	46.4 ± 0.4	43.9 ± 1.9[b]
(*R,R*)-**6**[a]	100 ± 1.9	52.0 ± 2.3	65.6 ± 1.8	63.7 ± 2.4	61.3 ± 1.9	51.7 ± 2.8	36.2 ± 2.4	31.3 ± 1.8

[a]Synthesis of falcarinol and falcarindiol analogues (*R*)-**3**, (*R*)-**4**, (*R*)-**5**, and (*R,R*)-**6** (see the Supporting Information). x ± s, *n* = 3. [b]**$p < 0.01$ vs control group.

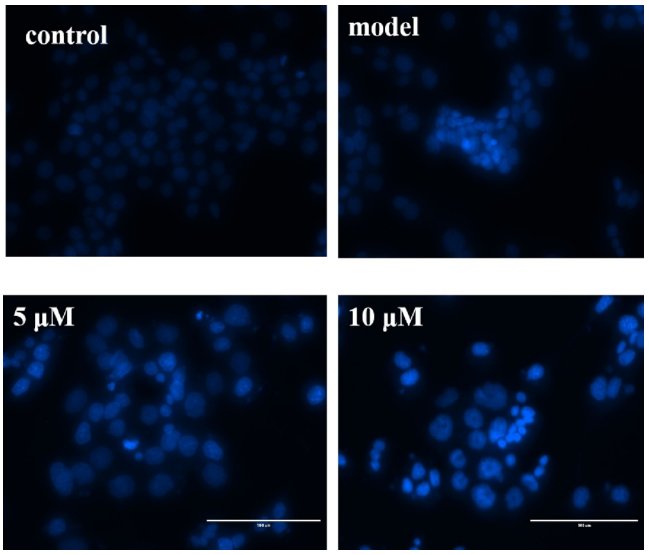

Figure 2. Apoptosis morphology of PC12 cells determined by Hoechst 33258 staining in the presence of 5 and 10 μM (*R*)-**2d**.

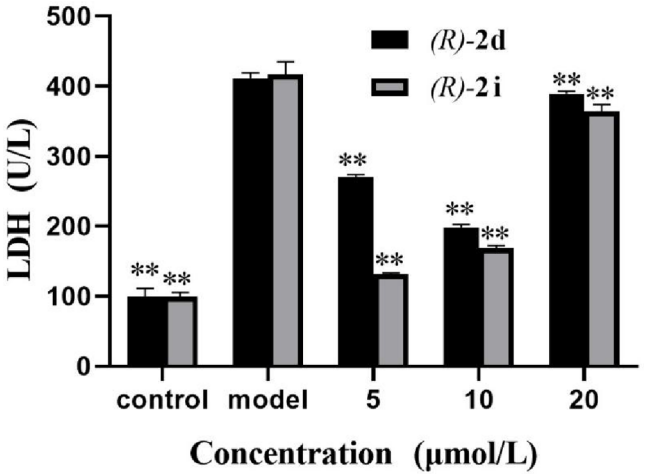

Figure 3. Effects of (*R*)-**2d** and (*R*)-**2i** on LDH release in NaN_3-induced PC12 cells (x ± s, *n* = 3; **$p < 0.01$ vs a model group). LDH activity for falcarinol (**1a**) at 4 μM was 211 U/L.

(53 and 47 nmol/mL, Table S6, Supporting Information), which shows their higher potential for oxidation resistance than falcarinol (**1a**) (68 nmol/mL). Furthermore, superoxide dismutase is the primary defense system to protect biological systems from oxidative stress. As shown in Figure 5, exposure of PC12 cells to NaN_3 in the model reduces significantly the activity of SOD (54 U/mg pro) as compared to the control group. However, the decrease of SOD activity was attenuated

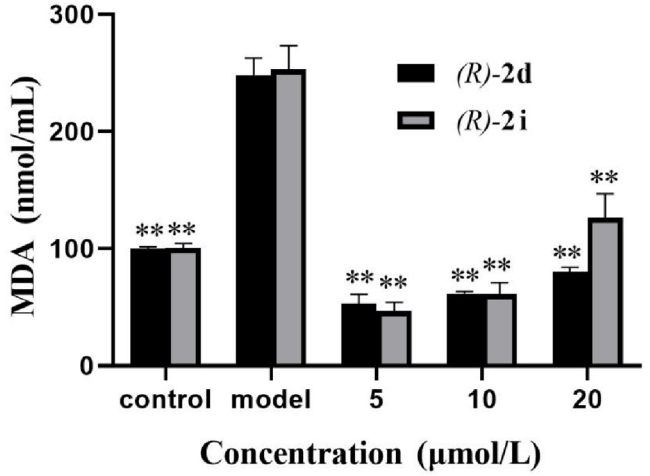

Figure 4. Effects of (*R*)-**2d** and (*R*)-**2i** on MDA in NaN_3-induced PC12 cells (x ± s, *n* = 3; **$p < 0.01$ vs model group). The MDA activity for falcarinol (**1a**) at 4 μM was 68 nmol/mL.

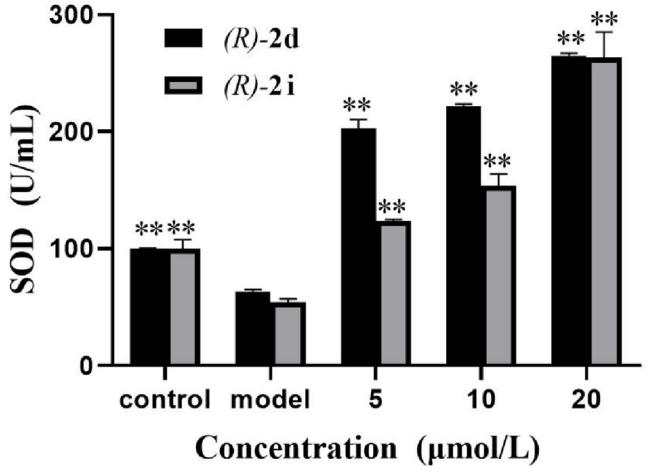

Figure 5. Effects of (*R*)-**2d** and (*R*)-**2i** on SOD in NaN_3-induced PC12 cells (x ± s, *n* = 3; **$p < 0.01$ vs a model group). The activity for falcarinol (**1a**) at 4 μM was 213 U/mg pro.

dose-dependently when PC12 cells were preincubated with analogues (*R*)-**2d** and (*R*)-**2i** at concentrations of 5−20 μM with 124−265 U/mg pro (Table S7, Supporting Information). These findings indicate that analogues (*R*)-**2d** and (*R*)-**2i** may protect PC12 cells against NaN_3-induced cell injury, mainly via increasing resistance to oxidative stress.

It was examined as to whether the protective effect of (*R*)-**2d** and (*R*)-**2i** on NaN_3-induced oxidative stress is due to their inhibition on the excessive production of intracellular free radicals generated by a ROS-dependent up-regulation of an

https://doi.org/10.1021/acs.jnatprod.1c00136
J. Nat. Prod. XXXX, XXX, XXX−XXX

endogenous antioxidant system. As shown in Figure 6, the exposure of PC12 cells to NaN_3 in the model resulted in a

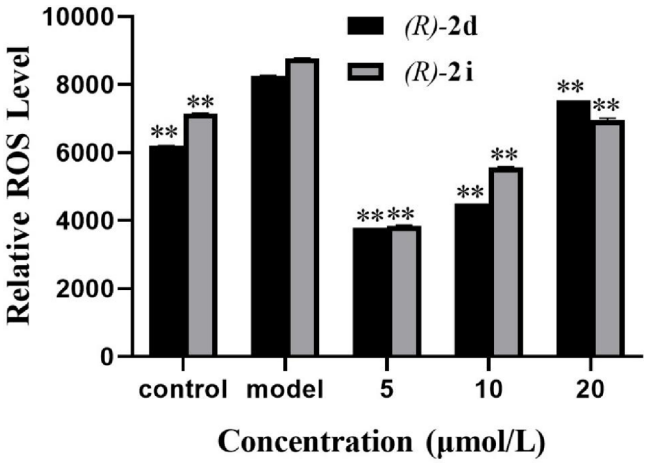

Figure 6. Effects of (*R*)-**2d** and (*R*)-**2i** on ROS level in NaN_3-induced PC12 cells as determined using flow cytometric analysis (x ± s, $n = 3$; $^{**}p < 0.01$ vs a model group). The ROS level for falcarinol (**1a**) at 4 μM was 5098.

significant increase of the ROS level (8250) in the PC12 cells, as determined using flow cytometric analysis and comparison to the control group (6197) (Table S8, Supporting Information). The increase of ROS levels could be attenuated significantly by pretreatment with analogues (*R*)-**2d** (3842) and (*R*)-**2i** (3794) at a concentration of 5 μM (Table S8, Supporting Information), which both exhibited a better resistance to oxidative stress than falcarinol (**1a**) (5098).

Calcium overload can activate calcium-dependent proteases and nitric oxide synthase, destroy mitochondria, and result in neuronal excitotoxicity.[23,24] These effects might derive from the formation of ion channels within the cell membrane by toxic fragments of fibril Aβ, fostering a direct leakage of calcium into cells.[25] Some studies have shown that several L-type calcium channel blockers may alleviate neuronal degeneration in early-stage AD therapy.[26,27] Therefore, in the above-mentioned mechanism investigation, the falcarinol-type analogues might act as targeted molecules for L-type calcium ion channels and play a blocking role in the upstream of the cell pathway. As shown in Figure 7, the L-type calcium channel-blocking activity of falcarinol (*R*)-**1a** and its analogue (*R*)-**2i** was found for the first time using the manual patch clamp technique on HEK-293 cells stably expressing *h*Cav1.2 (α1C/β2a/α2δ1). In the presence of 100 μM falcarinol (*R*)-**1a**, the membrane current ($I_{Ca\text{-}L}$) decreased to 38.4% of its original value, but was restored to 50.8% of this value after being washed out with the external solution (Figure 7B). In the presence of 100 μM (*R*)-**2i**, the $I_{Ca\text{-}L}$ value decreased to 20.3% of its original value but was not restored after being washed out (Figure 7D). These results showed that the inhibitory effect of falcarinol (*R*)-**1a** on the $I_{Ca\text{-}L}$ value was partially reversible, whereas its analogue (*R*)-**2i** irreversibly affected the $I_{Ca\text{-}L}$.

The time course of $I_{Ca\text{-}L}$ was changed progressively by the gradient concentrations of 10, 30, and 100 μM of falcarinol (*R*)-**1a** and its analogue (*R*)-**2i**, which acted rapidly on the L-type calcium channel (Figures S4–S6, Supporting Information). The inhibition rates by falcarinol (*R*)-**1a** at 10, 30, and 100 μM were 7.9 ± 3.2%, 28.1 ± 8.5%, and 61.6 ± 6.7%, respectively (Figure S6C, Supporting Information), while those of its analogue, (*R*)-**2i**, were 7.7 ± 2.4%, 38.6 ± 6.9%, and 79.7 ± 8.4%, respectively (Figure S6F, Supporting Information). These results showed that falcarinol (*R*)-**1a** and its analogue (*R*)-**2i** can inhibit rapidly the opening of L-type calcium channels in a concentration-dependent manner, with IC_{50} values of 67.3 and 41.3 μM. Thus, the mechanism of the neuroprotective effect of the falcarinol-type analogues may be correlated with L-type calcium channel-blocking activity by inhibiting calcium overload, which subsequently reduces cell apoptosis.

EXPERIMENTAL SECTION

General Experimental Procedures. All reactions were performed under inert gas conditions unless otherwise specified. Falcarinol [(*R*)-**1a**] was purchased from Shanghai YuanMu. Other chemicals were from commercial sources and were used directly without purification. Methylene chloride, tetrahydrofuran, and diethyl ether were purified by MBraun SPS-800-Systems, and the other solvents used were dried by standard methods prior to use. Optical rotations were obtained by using a Hanon P810/P850 automatic polarimeter with a sodium $\lambda = 589.3$ nm filter. The NMR data were recorded with a Bruker TM400 NMR spectrometer. HRMS (QTOF) were measured on a SCIES-X500r instrument. HPLC analyses were performed with a Waters 1525 apparatus using Diacel Chiralcel OD-H, Chiracel AD-H, and Chiralcel AS-H columns, with detection at $\lambda =$ 254 or 220 nm on a Waters 2487 instrument.

Synthesis, Isolation, and Purification of Falcarinol Analogues (2). A typical procedure for the asymmetric addition of diynes to aldehydes by using (*R*)- or (*S*)-BINOL is as follows: Under argon, Zn powder (5.1 mmol, 10.2 equiv) and (*R*)- or (*S*)-BINOL (0.34 mmol, 0.68 equiv) were added to a 25 mL flask equipped with a mechanical stirrer. Then, EtI (10.2 mmol, 20.4 equiv), $Ti(O^iPr)_4$ (0.85 mmol, 1.70 equiv), and an alkyne (1 mmol, 2 equiv) were added dropwise using a syringe. After 5 min, tetrahydrofuran (1 mL) was added, and the mixture was stirred at room temperature for 24 h. Then, diethyl ether (15 mL) was added, followed by the addition of an aldehyde (0.5 mmol, 1 equiv) after 1 h. The mixture was stirred for 12 h, and then it was quenched with aqueous saturated NH_4Cl (5 mL). The solution was extracted with CH_2Cl_2 (3 × 30 mL), and the combined organic phase was dried (Na_2SO_4), filtered, and concentrated under reduced pressure. The crude product was purified by column chromatography on silica gel to afford the desired compound **2**.

Culture of PC12 Cells. PC12 cells were provided by Shanghai Cell Bank of the Chinese Academy of Sciences. Cells were cultured in RIMP 1640 culture medium (Gibco) containing 10% inactivated fetal bovine serum (FBS, Sijiqing Biological Engineering Materials Co., Ltd., Hangzhou, People's Republic of China), penicillin (100 IU/mL), streptomycin (100 mg/mL), and L-glutamine (2 mmol/L) in a thermostatic incubator (Thermo) (setting: 37 °C, 5% CO_2). When the cell confluence reached 80–90%, cells were digested with 0.25% trypsin and passaged by a ratio of 1:3.

Cell Viability Assay by the CCK-8 Method. The viability of PC12 cells was determined using a cell counting kit-8 (CCK-8) assay (Dojindo Molecular Technologies, Inc., Kumamoto, Japan), according to the manufacturer's instructions. PC12 cells were cultured in 96-well plates at 37 °C under an atmosphere of 5% CO_2 and 95% air. At the end of the treatment, CCK-8 reagent (10 μL) was added to each well, and the plates were then incubated at 37 °C for 0.5 to 2 h in the incubator. Absorbance at a wavelength of 450 nm was measured with a Spectra Max M3 microplate reader (Molecular Devices, USA). The mean optical densities (ODs) from four wells in the indicated groups were used to calculate the cell viability, which was expressed as a percentage of the cell survival rate when compared with the control group. All experiments were performed in triplicate and repeated three independent times.

Establishment of a Model of PC12 Cell Injury Induced by NaN_3. The injury model was constructed in the following manner. In brief, the RPMI 1640 medium was removed, and PC12 cells were

https://doi.org/10.1021/acs.jnatprod.1c00136
J. Nat. Prod. XXXX, XXX, XXX−XXX

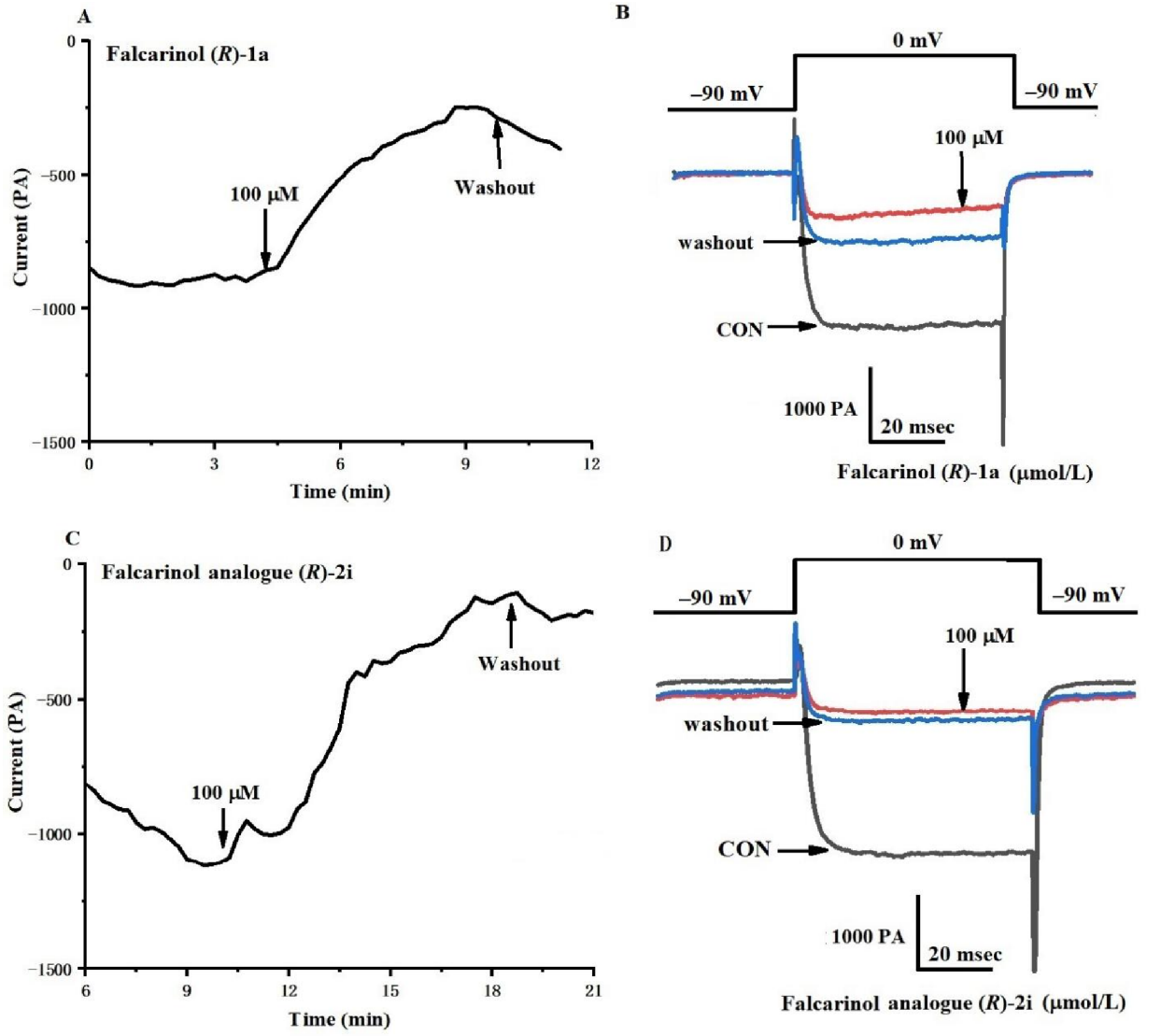

Figure 7. L-Type calcium channel-blocking activity of falcarinol (*R*)-**1a** and its analogue (*R*)-**2i** at a concentration of 100 μM. (A) Time course for (*R*)-**1a**. (B) Current traces for (*R*)-**1a**. (C) Time course for (*R*)-**2i**. (D) Current traces for (*R*)-**2i**.

washed twice with glucose-free Earle's balanced salt solution (PBS) at pH 7.5 and then maintained in glucose-free RPMI 1640 without FBS. Subsequently, neurotoxic damage was induced by adding the indicated concentration of NaN_3 to the cultured cells for 24 h.

Evaluation of Protective Effects of Falcarinol (1a) and Its Analogues (2). Cells were preincubated with the indicated concentrations of falcarinol (**1a**) and its analogues (**2**) for 1 h prior to NaN_3 treatment and maintained throughout the entire experiment. Falcarinol (**1a**) was dissolved in DMSO and was freshly prepared immediately prior to use. Analogues **2** were dissolved in absolute ethyl alcohol and were freshly prepared immediately prior to use. The stock solutions were added directly into the bath solution to achieve the final concentration. Control cultures were maintained in RPMI 1640 for the same duration under normoxic conditions. The concentrations of all the reagents were maintained throughout the injury period.

Hoechst 33258 Fluorescence Staining for Morphological Observations of PC12 Cell Apoptosis. PC12 cells in the logarithmic growth phase were taken and inoculated in a six-well culture plate at a density of about 1×10^5 cells per well. After culturing overnight at 37 °C and in a 5% CO_2 incubator, the medium was discarded, following treatment with NaN_3 for 24 h in the presence or absence of the 5, 10, and 20 μM falcarinol analogues, (*R*)-**2d** and (*R*)-**2i**, also including a control group and a model group. The cells were washed twice with PBS and fixed in 0.5 mL of methanol per well for 30 min. The fixed cells were incubated with 1 mL of Hoechest 33258 staining solution for 10 min at 37 °C in the dark. After removal of the staining solution, the cells were washed twice with PBS and then observed using a fluorescence microscope (FL CD12-002, AMG, USA), with an excitation wavelength of 350 nm and an emission wavelength of 461 nm. For cell counts, five random fields (about 100 cells each field) were observed per coverslip. The results were expressed as percentages of Hoechst-positive nuclei (condensed or fragmented) relative to the total number of nuclei counted per coverslip for each experimental condition.

LDH Release, MDA Content, and SOD Activity Assays. The content of LDH and the activity of SOD and MDA released into the medium were evaluated with commercial detection kits (NJJC Bio). In brief, the cells were ruptured using a ultrasonic cell disruptor and centrifuged at 10 000 rpm for 10 min at 4 °C. The supernatant of each well was transferred to a fresh flat-bottomed 96-well culture plate and processed further for enzymatic analysis, as per the manufacturer's instructions. Each experiment was repeated three times independently.

ROS Levels Detected by Flow Cytometry. Production of intracellular ROS was determined using the fluorescent probe dichlorofluorescein diacetate (DCFH-DA), which can cross cell

https://doi.org/10.1021/acs.jnatprod.1c00136
J. Nat. Prod. XXXX, XXX, XXX−XXX

membranes and is hydrolyzed subsequently by intracellular esterase to nonfluorescent DCFH (Beyotime Institute of Biotechnology). PC12 cells were seeded in a six-well plate, with a cell density of 1×10^5 cells/mL. Following treatment with NaN_3 for 24 h in the presence or absence of 5, 10, and 20 μM of the falcarinol analogues (*R*)-**2d** and (*R*)-**2i**, the culture medium was changed to fresh RPMI 1640 containing 10 μM DCFH-DA for 30 min in an incubator at 37 °C in the dark. After being washed three times with PBS, the cells were observed by flow cytometry (FCM), with an excitation wavelength of 488 nm and an emission wavelength of 535 nm. Each experiment was performed independently three times.

Electrophysiological Manual Patch Clamp Recordings. Extracellular solution (mM): CsCl 139, $BaCl_2$ 5, $MgCl_2$ 1, glucose 10, HEPES 10, pH = 7.4, and osmolarity 290−320 mOsm. Intracellular solution (mM): cesium methanesulfonate 108, EGTA 10, $MgCl_2$ 0.4, $CaCl_2$ 2, HEPES 24, Na-ATP 4, pH = 7.2, and osmolarity 280−310 mOsm. The extracellular solution was used to bathe the recorded cell, while the intracellular solution with amphotericin B was used to fill the recording pipet. The final concentration for amphotericin B was 250 μg/mL. Test compounds and nifedipine were dissolved in 100% ethanol or 100% DMSO to obtain stock solutions for different test concentrations. Then, the stock solutions were diluted further with the extracellular solution to achieve final concentrations for testing. The final ethanol or DMSO concentration was not more than 1.00% for all compound concentrations. HEK-293 cells stably expressing *h*Cav1.2 (α1C/β2a/α2δ1) calcium channels were used for this test. The cells were cultured in a humidified and air-controlled (5% CO_2) incubator at 37 °C and were induced by tetracycline (Sangon Biotech, T0422) at 1 μg/mL for 24 h before testing. All experiments were performed at 24 °C. The recorded cells were incubated in a chamber attached to an inverted microscope (Nikon Ti-S, Japan) with the external solution at a flow rate of 1 mL/min. The glass microelectrode resistance ranged from 2 to 4 MΩ after being filled with the pipet solution. After establishing the whole cell configuration (perforation for 10 min), membrane currents ($I_{Ca\text{-}L}$) were recorded by a manual patch clamp system (Axon Multiclamp 700B, Digidata 1440, Molecular Devices, USA) and filtered at 10 kHz, and Clampfit 10.7 software was used for the analysis. State-dependent voltage protocol: from a holding potential of −90 mV, the voltage was stepped to 0 mV for 50 ms after 1000 ms prepulses that evoked 20% of channels into an inactivated state. After this, the voltage was stepped back down to a −90 mV holding potential. This voltage command protocol was repeated continuously every 15 s during the test.

Statistical Analysis. All statistical analyses were conducted with SPSS statistical software 17.0. All the values are expressed as means ± standard error of the mean. The statistical significance of differences between groups was determined by one-way analysis of variance followed by Tukey's post hoc multiple comparison tests or a Student's *t* test (two means comparison), with $p < 0.05$ considered to indicate statistically significant differences. Each experiment consisted of at least three replicates per condition.

■ ASSOCIATED CONTENT

Supporting Information

The Supporting Information is available free of charge at https://pubs.acs.org/doi/10.1021/acs.jnatprod.1c00136.

Chemical name, synthetic yields, enantiomeric excess, optical rotation, spectral data, as well as NMR and HPLC spectra of all synthetic compounds (PDF)

■ AUTHOR INFORMATION

Corresponding Authors

Qin Wang − *Department of Medicinal Chemistry, School of Pharmacy and Key Laboratory of Medical Electrophysiology, Ministry of Education, School of Pharmacy, Southwest Medical University, Luzhou 646000, People's Republic of China*; orcid.org/0000-0001-9852-5347; Email: wq_ring@hotmail.com

Chun Zhang − *Department of Medicinal Chemistry, School of Pharmacy, Southwest Medical University, Luzhou 646000, People's Republic of China*; Email: zc83good@126.com

Authors

Yang Li − *Department of Medicinal Chemistry, School of Pharmacy, Southwest Medical University, Luzhou 646000, People's Republic of China*

Wan-Li Tan − *Department of Medicinal Chemistry, School of Pharmacy, Southwest Medical University, Luzhou 646000, People's Republic of China*

Kai Guo − *Key Laboratory of Medical Electrophysiology, Ministry of Education, School of Pharmacy, Southwest Medical University, Luzhou 646000, People's Republic of China*

Xiao-Wei Gao − *Key Laboratory of Medical Electrophysiology, Ministry of Education, School of Pharmacy, Southwest Medical University, Luzhou 646000, People's Republic of China*

Jun Wei − *Department of Medicinal Chemistry, School of Pharmacy, Southwest Medical University, Luzhou 646000, People's Republic of China*

Dong Yi − *Department of Medicinal Chemistry, School of Pharmacy, Southwest Medical University, Luzhou 646000, People's Republic of China*

Complete contact information is available at: https://pubs.acs.org/10.1021/acs.jnatprod.1c00136

Author Contributions

#Y.L. and W.-L.T. contributed equally and are joint first authors.

Notes

The authors declare no competing financial interest.

■ ACKNOWLEDGMENTS

This work was supported by the Sichuan Science and Technology Program (2019JDTD0016), the Program of the Education Department of Sichuan Province (14TD0017), and the Applied Basic Research Program of Science and Technology Department of Sichuan Province (2021YJ0114).

■ REFERENCES

(1) Christensen, L. P. *Recent Pat. Food Nutr. Agric.* **2011**, *3*, 64−67.
(2) Dawid, C.; Dunemann, F.; Schwab, W.; Nothnagel, T.; Hofmann, T. *J. Agric. Food Chem.* **2015**, *63*, 9211−9222.
(3) Christensen, L. P. *Molecules* **2020**, *25*, 2568.
(4) Christensen, L. P.; Brandt, K. In *Plant Secondary Metabolites: Occurrence, Structure and Role in the Human Diet*; Crozier, A., Clifford, M. N., Ashihara, H., Eds.; Blackwell: Oxford, UK, 2009; Chapter 5, pp 147−173.
(5) Wang, Z. J.; Nie, B. M.; Chen, H. Z.; Lu, Y. *Chem.-Biol. Interact.* **2006**, *159*, 58−64.
(6) Nie, B. M.; Yang, L. M.; Fu, S. L.; Jiang, X. Y.; Lu, P. H.; Lu, Y. *Chem.-Biol. Interact.* **2006**, *160*, 225−231.
(7) Nie, B. M.; Jiang, X. Y.; Cai, J. X.; Fu, S. L.; Yang, L. M.; Lin, L.; Hang, Q.; Lu, P. H.; Lu, Y. *Neuropharmacology* **2008**, *54*, 845−853.
(8) Leonti, M.; Casu, L.; Raduner, S.; Cottiglia, F.; Floris, C.; Altmann, K. H.; Gertsch, J. *Biochem. Pharmacol.* **2010**, *79*, 1815−1826.
(9) Wyrembek, P.; Negri, R.; Kaczor, P.; Czyżewska, M.; Appendino, G.; Mozrzymas, J. W. *J. Nat. Prod.* **2012**, *75*, 610−616.

(10) Czyżewska, M.; Chrobok, L.; Kania, A.; Jatczak, M.; Pollastro, F.; Appendino, G.; Mozrzymas, J. W. *J. Nat. Prod.* **2014**, *77*, 2671−2677.
(11) Wyrembek, P.; Lebida, K.; Mercik, K.; Szczuraszek, K.; Szczot, M.; Pollastro, F.; Appendino, G.; Mozrzymas, J. W. *Br. J. Pharmacol.* **2010**, *160*, 1302−1315.
(12) Wyrembek, P.; Negri, R.; Appendino, G.; Mozrzymas, J. W. *Eur. J. Pharmacol.* **2012**, *683*, 35−42.
(13) Elfawy, H. A.; Das, B. *Life Sci.* **2019**, *218*, 165−184.
(14) Calvo-Rodriguez, M.; Hernando-Pérez, E.; López-Vázquez, S.; Núñez, J.; Villalobos, C.; Núñez, L. *Int. J. Mol. Sci.* **2020**, *21*, 1549.
(15) Zhang, K.; Zhang, C.; He, Z. H.; Huang, J.; Du, X.; Wang, L.; Wei, S. P.; Pu, L.; Wang, Q. *ChemBioChem* **2018**, *19*, 2293−2299.
(16) Wang, L.; Shou, P. P.; Wei, S. P.; Zhang, C.; Li, S. X.; Liu, P. X.; Du, X.; Wang, Q. *Molecules* **2016**, *21*, 112.
(17) Wang, Q.; Pu, L. *Synlett* **2013**, *24*, 1340−1363.
(18) Chen, S.; Liu, W.; Wu, X.; Ying, J.; Yu, X. Q.; Pu, L. *Chem. Commun.* **2015**, *51*, 358−361.
(19) Trost, B. M.; Chan, V. S.; Yamamoto, D. *J. Am. Chem. Soc.* **2010**, *132*, 5186−5192.
(20) Turlington, M.; Du, Y.; Ostrum, S. G.; Santosh, V.; Wren, K.; Lin, T.; Sabat, M.; Pu, L. *J. Am. Chem. Soc.* **2011**, *133*, 11780−11794.
(21) Hardy, M.; Zielonka, J.; Karoui, H.; Sikora, A.; Michalski, R.; Podsiadly, R.; Lopez, M.; Vasquez-Vivar, J.; Kalyanaraman, B.; Ouari, O. *Antioxid. Redox Signaling* **2018**, *28*, 1416−1432.
(22) Singh, A.; Kukreti, R.; Saso, L.; Kukreti, S. *Molecules* **2019**, *24*, 1583.
(23) Zhao, X. Y.; Lu, M. H.; Yuan, D. J.; Xu, D. E.; Yao, P. P.; Ji, W. L.; Chen, H.; Liu, W. L.; Yan, C. X.; Xia, Y. Y.; Li, S.; Tao, J.; Ma, Q. H. *Front. Neurosci.* **2019**, *13*, 30.
(24) Wu, A. J.; Tong, B. C. K.; Huang, A. S.; Li, M.; Cheung, K. H. *Curr. Alzheimer Res.* **2020**, *17*, 329−343.
(25) Esteras, N.; Abramov, A. Y. *Cells* **2020**, *9*, 2135.
(26) Ishii, M.; Hiller, A. J.; Pham, L.; McGuire, M. J.; Iadecola, C.; Wang, G. *J. Neurosci.* **2019**, *39*, 8816−8825.
(27) Wang, Y. F.; Tang, H. D.; Yang, C. M.; Zhao, H. C.; Jian, C. D. *Life Sci.* **2020**, *243*, 117293.

https://doi.org/10.1021/acs.jnatprod.1c00136
J. Nat. Prod. XXXX, XXX, XXX−XXX